Holobiont Evolution: Model of Phage/Bacteria Dynamics With Implications for the Lytic to Lysogenic Transition

Joan Roughgarden[1 2]

January 3, 2023

Abstract

A critique of the delay-differential equation model of Cambell (1961) for the population dynamics of virulent phage and bacteria reveals the need for a new model. This paper introduces a new and simple model for the population dynamics of phage and bacteria that features infection of bacteria by Poisson sampling of viral particles from the environment and is developed in discrete time with a time step equal to the viral latency time

Density-dependent burst size does not lead to virus-bacteria coexistence whereas density-dependent viral absorption onto the bacterial surface is sufficient to produce virulent virus-bacteria coexistence.

The condition for transition from a lytic to lysogenic phase is derived as a "switch function". The virus switches from lytic to lysogenic when its population grows faster with prophage than with separate virions produced by lysis of the infected cell.

The switch function predicts temperate viral-bacteria dynamics in several environmental scenarios including environmental enrichment leading to microbialization, fluctuating environmental conditions that promote horizontal gene transfer (HGT), and the integration of prophage-containing bacteria into the microbiome of a eukaryotic host forming a functionally integrated tripartite holobiont.

Introduction

This paper introduces a simple mathematical model for the population dynamics of phage and bacteria. The first third of the paper provides a detailed account of the original Campbell (1961) model for virulent phage-bacterial population dynamics upon which much later work has been based. A critique of the Campbell model reveals the need for a new model. Thereafter, the paper develops a qualitatively new and simple mathematical model for phage-bacterial population dynamics that reveals the conditions for virulent phage and bacteria to coexist and for temperate phage to shift from a lytic to lysogenic life cycle. The implications of the model for process of virus-mediated horizontal gene transfer (HGT) and for the formation of three-level holobionts consisting of virus, microbe and host are developed. The terminology used in the phage-bacteria interaction is summarized in the Supplementary Material.

[1]Hawaii Institute of Marine Biology, University of Hawaii, joaner@hawaii.edu and Department of Biology, Stanford University, rough@stanford.edu, ORCID: https://orcid.org/0000-0002-6360-7964

[2]Keywords: bacteriophage, lytic, lysogenic, microbialization, HGT, tripartite holobiont, mathematical model.

Campbell Model of Virulent Phage-Bacteria Population Dynamics

Consider a population of bacteria open to infection by a population of virulent phage. The question is whether the bacteria and virulent phage can coexist.

Model: Delay-Differential Equations

To answer this question, Allan Campbell proposed a mathematical model for their population dynamics. The Campbell model (Campbell 1961) introduced features that have persisted in phage-bacteria models until the present day. The Campbell model is:

$$\frac{dN(t)}{dt} = r\,N(t)\left(1-\frac{N(t)}{K}\right) - c\,V(t)\,N(t) \tag{1}$$

$$\frac{dV(t)}{dt} = b\,c\,V(t-\tau)\,N(t-\tau) - c\,V(t)\,N(t) - d\,V(t) \tag{2}$$

where $N(t)$ is the number of bacteria at time t, $V(t)$ is the number of virus particles at time t, $N(t-\tau)$ is the number of bacteria at time $t-\tau$, $V(t-\tau)$ is the number of virus particles at time $t-\tau$, τ is a time lag, r is the bacterial intrinsic rate of increase, K is the bacterial carrying capacity within its environment, c is the rate of conversion of mass-action collisions between virus particles and bacteria into infections, b is the burst size, and d is the per capita disintegration rate of virus particles. (The Campbell model was originally written for a phage-bacteria system in a chemostat. Here the chemostat nutrient flow terms are omitted.)

The Campbell model is a pair of nonlinear delay-differential equations. The first term of Eq. 1 assumes the bacteria grow logistically in the absence of virus. The second term is the loss of bacteria from infection brought about by mass-action random collision of bacteria with virus particles. The first term in Eq. 2 is the production of new virus particles that depend on the collisions that took place τ units of time previously. The time lag, τ, called the latency, is the time needed for the infecting virus particles to manufacture and release new virus particles using the bacteria's nucleotide replication machinery. The next term indicates the loss of free virus particles from the infections taking place at the present time, t. Thus, the virus particles disappear for the duration of the latency period. After infecting bacteria at time $t-\tau$ they reappear at time t as newly minted virus particles.

The Campbell model treats the bacteria and virus as *two* separate populations—the model is for their coupled population dynamics. This type of model is distinguished from those used in epidemiology that pertain to a *single* population containing multiple classes. Typically, a single host population is envisioned to consist of three classes—those susceptible, infected and resistant to some disease. These models are called SIR models (Kermack and McKendrick 1927, Anderson and May 1979). The time units in SIR models pertain to the time course of the disease in the

host, say days to months, whereas the time units in the Campbell model relate to the kinetics of bacterial and viral replication, say minutes. The SIR models typically feature infection resulting from mass action collisions between two classes of hosts—those infected and those susceptible, and not collisions of hosts directly with viruses. No time lags are included. The SIR models typically lead to three ordinary differential equations for the number of hosts in each disease class. For a mildly deleterious disease, the host population size is taken as constant, so that the three equations boil down to two equations for the fraction of hosts in two disease classes (*c.f.* Roughgarden, 1998, p. 302 *ff*). Some models have been proposed for marine virus and also for bacteria in chemostats that are hybrids between the Campbell-type population model and an SIR epidemiology model (Beretta and Kuang 1998, 2001, Bull *et al*. 2006). The discipline of epidemiology now has variants of SIR models tailored to a great many diseases (*cf.* Keeling and Rohani 2008, Diekmann *et al*. 2013, Bjørnstad 2018.) Thus, the Campbell model differs from the SIR family of epidemiological models by focussing on the virus and bacteria as distinct populations whereas SIR models focus solely on the infection status of one population—the host.

Equilibrium Coexistence of Virus and Bacteria

The equilibrium point of virus-bacteria coexistence in the Campbell model, $(\hat{N}, \hat{V})$, is found by setting $dN(t)/dt = 0$, $dV(t)/dt = 0$, $\hat{N} = N(t) = N(t-\tau)$, and $\hat{V} = V(t) = V(t-\tau)$ in Eqs. 1 and 2 yielding

$$\hat{N} = \frac{d}{(b-1)\,c} \tag{3}$$

$$\hat{V} = \frac{r\big((b-1)\,c\,K - d\big)}{(b-1)\,c^2\,K} \tag{4}$$

The equilibrium point is independent of the latency time, τ, although τ does influence the stability of the equilibrium. The condition for a feasible equilibrium point of coexistence between virus and microbe is read off from the numerator of Eq. 4 as

$$(b-1)\,c\,K > d \tag{5}$$

This condition means the birth of virus has to exceed the death of virus. This condition can always be satisfied if K is large enough. Specifically, the bacterial carrying capacity, K, must exceed

$$K_{\min} = \frac{d}{(b-1)\,c} \tag{6}$$

for the virus and bacterial populations to have positive equilibrium values. In fact, $K_{\min}$ works out to be the same as $\hat{N}$. Therefore, K must merely be greater than the bacterial abundance expected in the presence of the virus for the equilibrium in Eqs. 3 and 4 to be positive. The $\hat{N}$ is

Table 1: Example Parameters in Campbell Model

r	0.0347
K	10^8
τ	15
b	40
c	10^{-4}
d	0.693

independent of r and K, indicating that its abundance is controlled by the virus' parameters. The $\hat{V}$ does depend on r and K, and increases with the bacteria's r and decreases with the bacteria's K. This dependence of the bacterial abundance on the properties of the virus and of virus abundance on properties of the bacteria is a well known property of ecological predator-prey models (*c.f.* Roughgarden, 1998, p. 266 *ff*).

Order-of-magnitude guesses at parameter values for the model may be constructed from the literature. Consider the parameters for bacterial logistic growth, r and K. In the laboratory, the doubling time of *E. coli* is 20 minutes although it can be much slower in the wild (Gibson *et. al.* 2018). Assuming time units of minutes, this laboratory doubling time corresponds to $r = 0.0347$ (*i.e.* $0.0347^{20} = 2.00$). Next, in the human gut, which is the habitat of *E. coli*, this bacterium is typically present in 10^6 colony forming units per gram of stool (Foster-Nyarko and Pallen 2022). A typical value for the amount of faeces in a human is one lb or 450 grams (Alexa Answers, Amazon, retrieved July 21, 2022). So, a possible value for K is 10^8.

The time between the viral adsorption and first appearance of viral progeny is 10–15 minutes (Endy *et al.* 1997, Purohit *et al.* 2005). So, a possible value for the latency, τ, is 15 minutes.

The burst size from microbes infected with about two virus is about 80 virus particles (Gadagkar and Gopinathan 1980, Figure 4), so b will be taken as 40.

About one in 10^3–10^4 collisions between a virus and bacterium lead to a specific binding between the cellular receptor and the virus attachment protein on the surface of the virus (Philipson 1983). So in the model c is taken as 10^{-4}.

The half-life of free infectious influenza A virus is ≈ 3 hours (Baccam et al 2006). If the half life is taken on the order of 1 hour, the disintegration rate of free virus, d, works out to be about 0.693 (*i.e.* $d = -\ln(1/2)$).

These guesses at plausible parameter values are summarized in Table 1. Using these parameters, the equilibrium from Eqs. 3 and 4 at which bacteria and virulent virus coexist out to

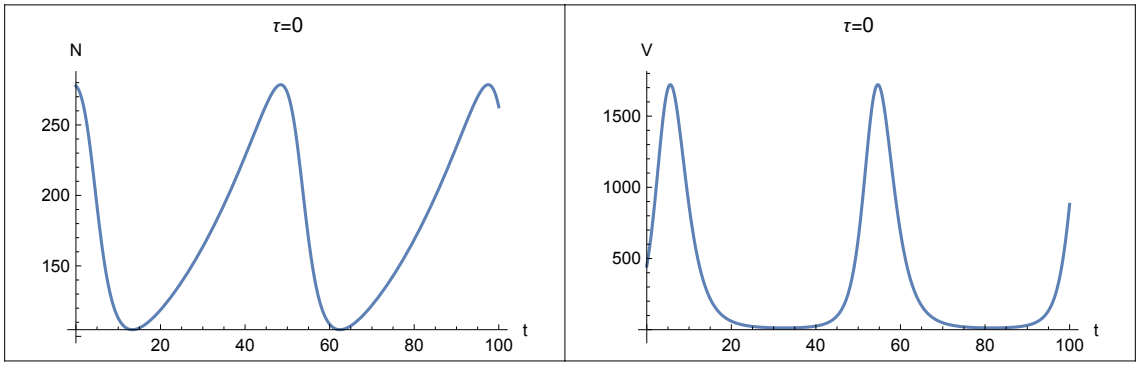

Figure 1: *Virus-Bacteria oscillation from the Cambell model with parameters from Table 1 excepting* $\tau = 0$. *Left is number of bacteria* vs. *time and right is number of virus* vs. *time. Initial conditions are* $N(0) = \hat{N} + 100$ *and* $V(0) = \hat{V} + 100$. *The period of the oscillation is about 55 minutes. Integration is from t = 0 to 100 minutes.*

be

$$\hat{N} = 177.692 \tag{7}$$

$$\hat{V} = 346.999 \tag{8}$$

Stability of Equilibrium with No Latency, $\tau = 0$

The coexistence of bacteria and a virulent virus require both that the equilibrium solutions for $\hat{n}$ and $\hat{v}$ from Eqs. 3 and 4 be positive *and* that the equilibrium point be stable to perturbations.

To begin, assume that the latency, τ, is 0, indicating an instantaneous conversion of virus infections into newly released virus particles. This assumption converts the Campbell model from a pair of delay-differential equations into a pair of ordinary differential equations that can be analyzed with conventional methods. The details are recorded in the Supplementary Material.

With $\tau = 0$, the equilibrium is always stable. The trajectories reveal a virus-bacteria oscillation through time that winds in to the equilibrium point. The period of the oscillation is determined by d and r, independent of b, c and K. The oscillation speeds up as d and/or r are increased. A high K diminishes the stability of the virus-bacterial equilibrium point.

The Campbell model, Eqs. 1 and 2, with $\tau = 0$ can be integrated with the NDSolve[] function in *Mathematica*. The solutions appear in the time domain as a nearly endless virus-bacteria oscillation as illustrated in Figure 1 and in a parametric plot as a nested set of loops, each representing a different initial condition, as illustrated in Figure 2. If the bacterial carrying capacity within the host is arbitrary set lower than 10^8, say approaching $K_{\min}$ from Eq. 6, then

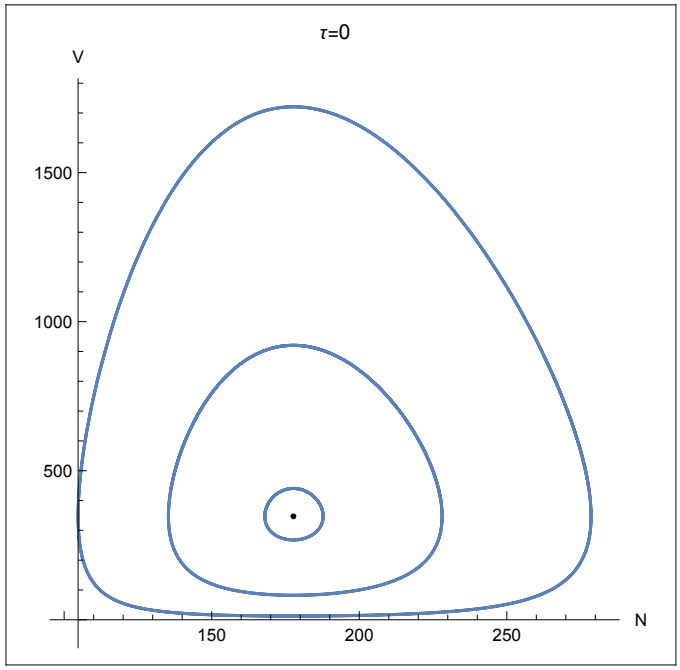

Figure 2: *Parametric plot of the Cambell model with parameters from Table 1 excepting* $\tau = 0$. *Horizontal axis is number of bacteria, vertical axis is number of virus, dot in center is the equilibrium point,* $(\hat{N}, \hat{V})$. *Outer loop was started at* $(N(0) = \hat{N} + 100,\ V(0) = \hat{V} + 100)$, *middle loop started at* $(N(0) = \hat{N} + 50,\ V(0) = \hat{V} + 50)$, *and inner loop started at* $(N(0) = \hat{N} + 10,\ V(0) = \hat{V} + 10)$. *Integration is from t = 0 to 100 minutes.*

the equilibrium becomes increasingly stable and the trajectories more rapidly spiral into the equilibrium point (not illustrated).

Stability of Equilibrium with Latency, $\tau > 0$.

The introduction of the latency time lag, τ, destabilizes the equilibrium at which virus and bacteria coexist. Although stability conditions for a system of delay-differential equations cannot generally be analyzed mathematically, the NDSolve[] function in *Mathematica* can successfully numerically integrate the Campbell model with a fixed time lag, τ. The left side of Figure 3 shows the parametric plot of virus and bacteria through 150 minutes with a small latency, $\tau = 1$ minute. The virus and bacteria populations were started toward the right of the equilibrium point, at $N(0) = \hat{N} + 100$ and $V(0) = \hat{V} + 100$, respectively. The trajectories wind out from the initial condition, spiraling ever farther from the equilibrium point.

The dynamic instability caused by the latency period becomes even worse with the realistic latency period of $\tau = 15$ minutes, as was recorded in Table 1. The right side of Figure 3 shows

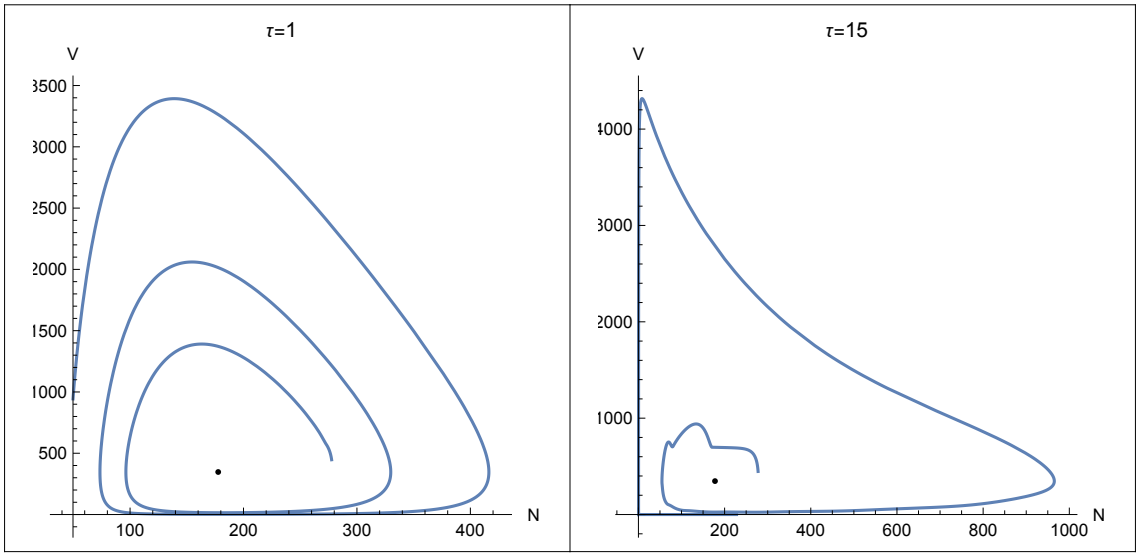

Figure 3: *Left: Parametric plot of the Cambell model with parameters from Table 1 excepting latency, $\tau = 1$ minute. Right: Parametric plot of the Cambell model with parameters from Table 1. Horizontal axis is number of bacteria, vertical axis is number of virus, dot in center is the equilibrium point, $(\hat{N}, \hat{V})$. Initial condition is $(N(0) = \hat{N} + 100,\ V(0) = \hat{V} + 100)$. Integration is from t = 0 to 150 minutes on the left and to 400 minutes on the right.*

the parametric plot of virus and bacteria through 400 minutes for a 15 minute latency. The virus and bacteria populations were again started toward the right of the equilibrium point, at $N(0) = \hat{N} + 100$ and $V(0) = \hat{V} + 100$, respectively. The trajectories show a jagged start because the initial condition for a delay-differential equation should specify the value of the variables at time $t = 0$ *and* at all times in the past until $t = -\tau$. Because the value of the variable is unknown before $t = 0$, the value at $t = 0$ is attributed to the earlier times. After a while, the trajectory catches up with its history and the trajectory smooths out. Thereafter the trajectories wind out and quickly hug the axes.

Campbell in 1961 may not have been aware of the destabilizing role of the viral latency period. At that time he wrote "If a virulent phage and a susceptible bacterium are mixed in an open growth system, such as a chemostat, one expects that, in general, the concentration of the two will approach some stable steady state value." (Campbell 1961, p157–8). But twenty years later, in 1981, he wrote that "Stable coexistence of phage and bacteria in chemostats has been verified experimentally. Comparison of theory with experiment revealed one discrepancy: Although the concentrations of bacteria and phage stabilized at approximately the predicted values, theoretical analysis and computer simulations predicted unstable oscillation rather than a stable steady state." (Campbell 1981, p. 61). Indeed, researchers testing a version of the Campbell

model with chemostats in 1977 wrote, "the time lag due to the latent period of the phage has a destabilizing effect which may be stronger than the opposite, stabilizing, effect of [bacterial population] regulation (Levin *et. al*. 1977, p. 11).

Critique of Campbell Model

Fifty-six years after the ground-breaking Campbell (1961) model appeared, Krysiak-Baltyn *et al.* (2017) published an extensive review of models for virulent phage and bacteria. They observed that "The basic model initially suggested by Campbell, and later refined by Levin and colleagues, has remained in use since first publication. Later studies have mostly made minor adjustments to the existing model to study dynamic behavior." (p. 964) They further observed that "Earlier studies on simple chemostat models indicated that the dynamics of the model are not in good quantitative agreement with experimental data. In particular, the stability of the simulated models is lower than expected, with many exhibiting heavy oscillations and extinction events where stable steady-states exist experimentally. Mechanisms could account for this stability have been proposed and explored to some extent. These mechanisms include spatial heterogeneity (where variations of concentration create pockets where bacteria can be more shielded from phage infection), distributed latency time or burst size, variable adsorption rate which varies as a function of either cell density or growth rate or due to switches in the phenotypic states of bacteria." (p. 964) They note that "Models that incorporate other kinetics describing bacterial growth other than those included in this review are lacking" (p. 965). Krysiak-Baltyn *et al.* (2017) conclude that "On a practical level, the usefulness of computational models of bacteria and phages has not yet been established. The simpler chemostat models may first need to become more accurate" (p. 965).

The premise of this paper is that improving the original Campbell model by adding more details has been repeatedly tried and failed and that the original Cambell model should be set aside and replaced by a newly conceptualized model. One needed change is to set aside the assumption of mass-action kinetics for viral infection (*i.e.*, infection rates equal to the product of bacterial numbers with viral numbers, $N \times V$) because this formula rules out incorporating density dependence in viral absorption and viral production. Instead, infection should be modeled as a Poisson colonization process, as experimentally established years ago by Ellis and Delbrück (1939). The other needed change is to abandon delay-differential equations whose time delays many researchers have simply evaded by letting the latency period equal zero. Instead, the model should be framed in discrete time with the time step being the latency period, not unlike using the generation time of a macro-organism as a time step.

All in all, the Campbell (1961) model should be set aside for three reasons. First, it predicts instabilities to virulent virus-bacteria population dynamics that are contradicted experimentally. Second, the Campbell (1961) is so mathematically challenging that its use is impractical in bi-

ology. How to mathematically analyze a system of nonlinear delay differential equations is an ongoing subject of research in applied mathematics (Tang and Zou 2008, Huang et. al. 2010). And third, the form of the Campbell model discourages its extension as part of a larger model for three-tier holobionts consisting of virus, bacteria and multicellular host.

More generally, one may ask whether the qualitative picture of virus-bacteria dynamics is the correct picture. The Campbell model envisions that virus-bacteria population dynamics involves two counteracting forces—the stabilizing force of density-dependent bacterial population growth and the destabilizing force of time lags arising from the virus latency period. The outcome is a balance of these forces. According to the Campbell model, small mammals should have fewer types of phage infecting bacteria than large mammals because the low K for bacteria in their small guts precludes the coexistence of many types of phage according to Eq. 6. Conversely, large mammals should support more types of phage infecting their bacteria because the large K for bacteria in their large guts allows more types of phage to satisfy Eq. 6. However, any phage-bacteria coexistence in large mammals may be temporary because the weakened density dependence from a large K should lead to large virus-bacteria oscillations. No evidence exists to support these qualitative predictions. In short, the Campbell model describes a situation that simply is not what is going on. Instead, a new picture of virus-bacteria population dynamics is needed, one that locates the equilibrium point and its stability within the virus-bacteria interaction itself without appealing to an external carrying capacity to stabilize the overall virus-bacteria system.

New Model for Virulent Phage-Bacteria Population Dynamics

Figure 4 (Left) offers a diagram of a virulent virus-bacteria life cycle as the basis for a new system of equations describing virus and bacteria population dynamics. The model is defined in discrete time with the time step being the viral latency period. A time step begins with the state variables, $N(t)$ and $V(t)$ for the number of bacteria and free virus particles (virions) in their environmental source pools at time t. Then the virus infect the uninfected bacteria according to a Poisson distribution such that some bacteria remain uninfected, some have only one infection, some have two infections *etc*. as depicted in the diagram (Ellis and Delbrück 1939). Poisson sampling was previously employed in models by Roughgarden (2020, 2023), continuing the framing presented in Roughgarden et al (2018)

The Poisson distribution describing the infection process has density parameter, $\mu(t) \equiv a(v(t))\, v(t)$ where $v(t) \equiv V(t)/N(t)$ is the ratio of virus to bacteria in their source pools. The $a(v(t))$ is the adsorption function—it refers to the probability that a viral particle comes in contact with a bacterium and binds to surface molecules for subsequent incorporation into the bacterial

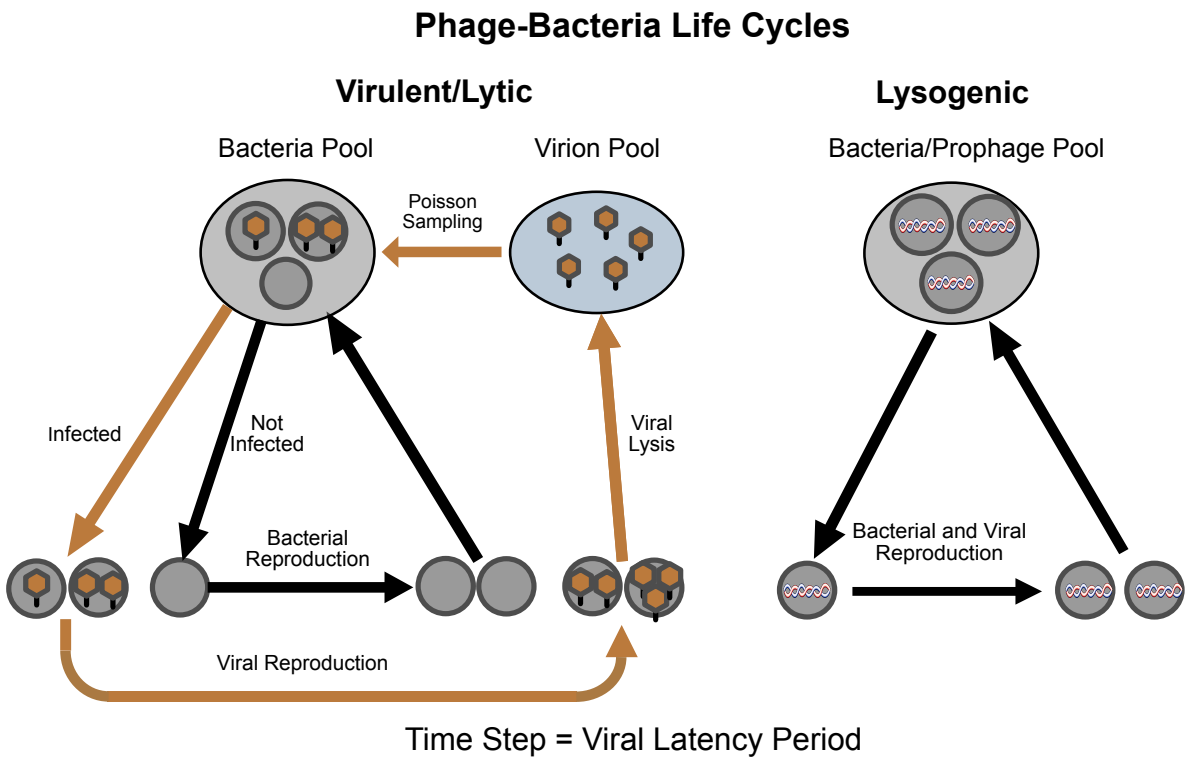

Figure 4: *Phage-bacteria life cycles. Left: life cycle for virulent phages and for the lytic phase of temperate phages. Bacteria in the bacterial source pool in the environment are infected by free virus particles (virions) from the viral source pool according Poisson sampling. The infected bacteria are the site of viral replication, leading to the release of new virions and the death of the infected cells. The uninfected bacteria replicate to produce more bacteria available for infection to begin the next time step. Right: life cycle for a temperate phage in its lysogenic phase. The virus is represented as a helix that is incorporated as a prophage into the genome of its bacterial host. The virus life cycle is coincident with the bacterial life cycle. The time step is the viral latency period.*

cell. Adsorption is a function of $v(t)$ because the number binding sites on the surface of the bacterium is finite and the sites may become saturated. Thus, $a(v(t))$ includes information about the binding affinity of virus particles to receptors in the bacterial surface and also about the number of binding sites. Furthermore, $a(v(t))$ also includes information about the accessibility of the bacterium to virus particles. For a given ratio of virus to bacteria, $v(t)$, if the environment is such that virus are prevented from reaching the bacteria, then $a(v(t))$ is low compared to $a(v(t))$ in environments that allow ready access of the virus to the bacteria. Environments may differ in how viscous the media is, or for airborne virus particles, whether air filters are installed.

Model: Recursion Equations in Discrete Time

According to a Poisson distribution, the fraction of uninfected bacteria that remain uninfected, $P_0(\mu(t))$, is $e^{-\mu(t)}$ and the fraction of bacteria colonized by m virus, $P_m(\mu(t))$, is $\frac{e^{-\mu(t)}\mu(t)^m}{m!}$ for $m \geq 0$ where $\mu(t) = a(v(t))\, v(t)$. The m indexes the number of virus per bacterium. The fraction of bacteria that are infected by one or more virus is $1 - P_0(\mu(t))$.

The uninfected bacteria population increases by a geometric factor of increase per time step, R. Necessarily, $R > 1$, for the bacteria to be able to increase in the absence of the virus. The R is related to the continuous time intrinsic rate of increase, r, in the Campbell model as $R = 1 + e^{r\,\tau}$ where τ is the length of a time step, *i.e.* the viral latency period. Accordingly, the uninfected bacteria resupply the bacterial source pool as

$$N(t+1) = R\, P_0(\mu(t))\, N(t) \tag{9}$$

where $P_0(\mu(t))$ is the Poisson probability that a bacterium is uninfected.

Next, the virus in the infected bacteria produce new virus particles as

$$\begin{aligned} V(t+1) &= \Big(b(1)\, P_1(\mu(t)) + b(2) P_2(\mu(t)) + \dots\Big)\, N(t) \\ &= \Big(\sum_{m=1}^{\infty} b(m)\, P_m(\mu(t))\Big)\, N(t) \end{aligned} \tag{10}$$

where $b(m)$ is the burst size from a bacterium infected with m virus particles and $P_m(\mu(t))$ is the Poisson probability that a bacterium is infected by m virus particles. More succinctly,

$$V(t+1) = \widetilde{b}(\mu(t))\, N(t) \tag{11}$$

where

$$\widetilde{b}(\mu(t)) \equiv \sum_{m=1}^{\infty} b(m)\, P_m(\mu(t)) \tag{12}$$

and $\widetilde{b}(\mu(t))$ is the cumulative burst per bacterium from all the infected bacteria at time t.

Eqs. 9 and 10 together constitute a new population-dynamic model for virulent virus and bacteria populations based on the life cycle sketched in Figure 4 (Left). The parameters in the model are R, the geometric factor of increase for uninfected bacteria, $a(v)$, the adsorption function, and $b(m)$, the burst-size function.

The model may be simplified by dividing Eq. 11 by Eq. 9

$$\frac{V(t+1)}{N(t+1)} = \frac{\widetilde{b}(\mu(t))\, N(t)}{R\, P_0(\mu(t))\, N(t)}$$

Then identify $v(t+1)$ with $\frac{V(t+1)}{N(t+1)}$ and $v(t)$ with $\frac{V(t)}{N(t)}$ yielding

$$v(t+1) = \frac{\widetilde{b}(\mu(t))}{R\, P_0(\mu(t))} \tag{13}$$

Equation 13 is a dynamical equation in one variable, $v(t)$, where $\mu(t) = a(v(t))\, v(t)$.

This paper separately explores the possibility of phage-bacteria coexistence with a density-dependent burst size, $b(m)$, and with a density-dependent absorption, $a(v)$. The case of no density dependence is also provided for comparison.

Density-Dependent Burst Size

Several choices are available for the burst size from a bacterium as a function of the number of virus in it, $b(m)$. The burst size might increase linearly with m so that $b(m) = b_o\, m$ where b_o is the contribution to the overall burst made by a single viral particle (Patel and Rao 1984, Figures 1–2). Alternatively, $b(m)$ might be a constant, $b(m) = b_o$, indicating that the burst size does not increase for m beyond the initial infection. A constant $b(m)$ indicates strong density dependence and is consistent with surveys reporting that burst sizes are characteristic of various viral taxa (Parada *et al.* 2006, Ranasinghe 2019). Another possibility is to assume $b(m)$ is a convex increasing function of m (Gadagkar and Gopinathan 1980, Figures 4–5). In this case, the burst-size function might be taken as $b(m) = b_o\, m^{\alpha}$ where α is an exponent between 0 and 1, say 1/2. A final possibility is to allow α to be negative, say $\alpha = -1$, to indicate that burst size varies inversely with the multiplicity of infection, indicating extremely strong density dependence as a response to "superinfection" (Brown and Bidle 2014). These possible relations between burst size and m may be subsumed by taking $b(m) = b_0\, m^{\alpha}$ with α as 1, 1/2, 0, or -1. Here, the cases of $\alpha = 1$ and $\alpha = 0$ will be investigated analytically. Results (not shown) for other α are similar.

Density-Dependent Absorption

The molecular biology of viral absorption onto the surface of bacterial and animal cells has been the focus of much recent study (Dimitrov 2004, Grove and Marsh 2011, Yamauchi and Helenius 2013, Maginnis 2018, Koehler *et al.* 2020, Huss *et al.* 2021). The kinetics of virus binding to cell surface has also been investigated (Moldovan *et al.* 2007, Hubbs *et al.* 2019, Echeverría-Vega *et al.* 2020, Koonjan *et al.* 2022). These studies are consistent with the assumption that the binding sites for virus on the surface of a bacterium become saturated as the density of viral particles increase. Accordingly, the absorption function will be taken as $a(v(t)) = a_o\,(1 - \frac{v(t)}{\kappa})$ where κ is the saturation density—the viral density at which all the binding sites per bacterium are occupied and a_o is the maximal probability of binding when all the binding sites are available. Also, it is required that $0 \leq v(t) \leq \kappa$. This formula postulates that the probability of a viral particle binding to a bacterium tends to zero as the binding sizes fill up, and equals zero when the viral density, v, equals κ.

Table 2: Example Parameters in New Model

Time Step	15 min
R	2
b_o	40
a_o	0.1
κ	2 to 20, Increment 2

Models with Density-Dependent Burst Size or Absorption

Illustrations are offered of the effectiveness of density dependence with either burst size or absorption probability. The case of no density dependence is also presented for comparison.

Parameters

Order of magnitude guesses for parameter values approximately follow those used previously for the Cambell (1961) model. The time step, which is the latency period, is 15 minutes, implying four steps per hour. Using the Campbell value for r would lead to a geometric factor of bacterial population growth per time step, R, of 2.68 *i.e.* $(1 + e^{0.0347 \times 15})$. For simplicity, here R is taken as 2. As before, the burst size, b_o is taken as 40. The base viral absorption coefficient, a_o is arbitrarily taken as 0.1. For the case with density-dependent absorption, κ is arbitrarily taken as 2 to 20 with a increment of 2. These parameters are summarized in Table 2.

Case 1, No Density Dependence: $a(v(t)) = a_o$**,** $b(m) = b_o\, m$

Here,

$$\mu(t) = a_o\, v(t) \tag{14}$$

and, upon doing the summation[3] in Eq. 12 ,

$$\widetilde{b}(\mu(t)) = b_o\, a_o\, v(t) \tag{15}$$

so Eq. 13 becomes

$$v(t+1) = \frac{b_o}{R}\, \frac{a_o\, v(t)}{e^{-a_o\, v(t)}} \tag{16}$$

Case 2, Density-Dependent Burst Size: $a(v(t)) = a_o$**,** $b(m) = b_o$

Here,

$$\mu(t) = a_o\, v(t) \tag{17}$$

[3] *cf.* Poisson summation identities in Supplementary Material

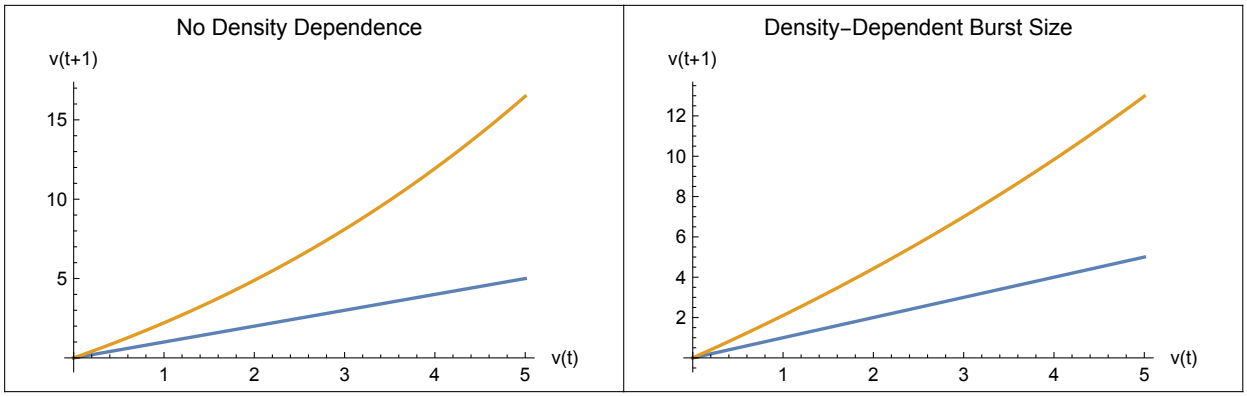

Figure 5: $v(t+1)$ *vs.* $v(t)$*, in brown, for no density dependence (left) and for a density-dependent burst size (right) from Eqs. 16 and 19. The diagonal line, in blue, indicates* $v(t+1) = v(t)$*. An intersection of the brown curve with the blue line would indicate an equilibrium point where virus and bacteria coexist, provided the equilibrium is stable. Because the curve does not intersect the line in either plot, no coexistence occurs in either case. Here,* $a_o = 0.1$*,* $b_o = 40$*, and* $R = 2$

and, upon doing the summation in Eq. 12,

$$\widetilde{b}(\mu(t)) = b_o\,(1 - e^{-a_o\,v(t)}) \tag{18}$$

so Eq. 13 becomes

$$v(t+1) = \frac{b_o}{R}\,\frac{1 - e^{-a_o\,v(t)}}{e^{-a_o\,v(t)}} \tag{19}$$

A point of possible coexistence occurs at the value of v for which $v(t+1)$ equals $v(t)$. This condition is shown graphically in Figure 5. An intersection of the curve for $v(t+1)$ with the line for $v(t+1) = v(t)$ would indicate an equilibrium point for possible virus-bacteria coexistence. The curve and line do not intersect in either case. Therefore coexistence, not surprisingly, is impossible without any density dependence, but surprisingly, is also impossible if the density dependence is solely in the burst size.

Case 3, Density-Dependent Absorption: $a(v(t)) = a_o\,(1 - \frac{v(t)}{\kappa})$**,** $b(m) = b_o\,m$

Here,

$$\mu(t) = a_o\,(1 - \frac{v(t)}{\kappa})\,v(t) \tag{20}$$

and, upon doing the summation in Eq. 12,

$$\widetilde{b}(\mu(t)) = b_o\,a_o\,(1 - \frac{v(t)}{\kappa})\,v(t) \tag{21}$$

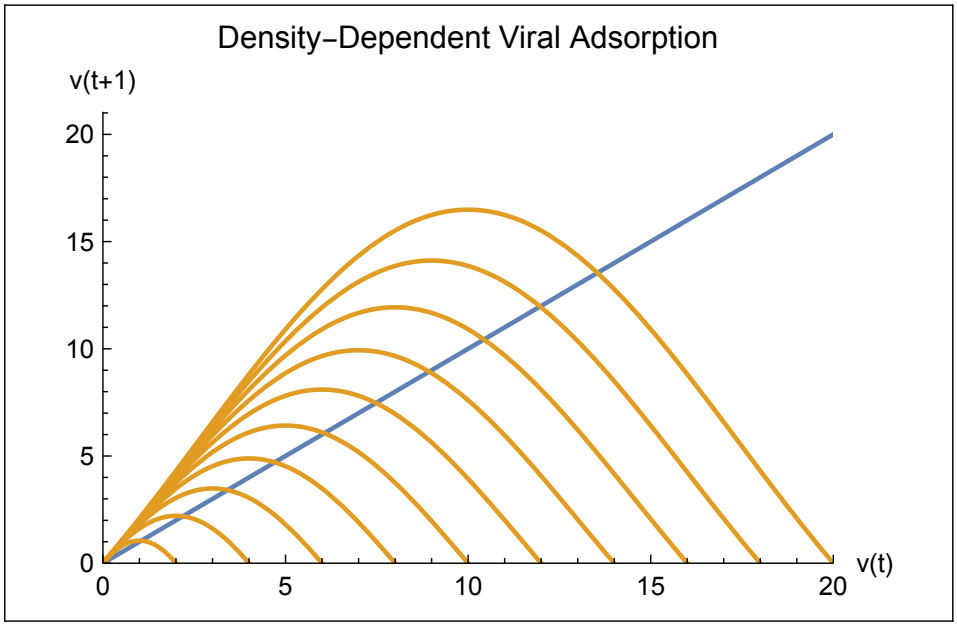

Figure 6: $v(t+1)$ *vs.* $v(t)$*, in brown, for density-dependent absorption from Eq. 16 and 22. The diagonal line, in blue, indicates* $v(t+1) = v(t)$*. The intersection of the brown curve with the blue line indicates an equilibrium point where virus and bacteria coexist provided the equilibrium is stable. Here,* $a_o = 0.1$*,* $b_o = 40$*,* $R = 2$*, and* κ *varies left to right from 2 to 20 in steps of 2.*

so Eq. 13 becomes

$$v(t+1) = \frac{b_o}{R} \frac{a_o \left(1 - \frac{v(t)}{\kappa}\right) v(t)}{e^{-a_o \left(1 - \frac{v(t)}{\kappa}\right) v(t)}} \tag{22}$$

Figure 6 shows the curve $v(t+1)$ and the line for $v(t+1) = v(t)$ with density-dependent absorption for several values of the saturation density, κ based on the parameter values in Table 2. The curves intersects the line indicating equilibrium points, $\hat{v}$, at which virus and bacteria can coexist, providing the equilibrium points are stable, as analyzed further in the next section. The equilibrium points, $\hat{v}$, increase with increasing saturation densities, κ. Moreover, the slope of the $v(t+1)$ curve at the intersection point is always negative and become steeper as κ increases.

Because the evidence shows that density dependence in burst size is weak to begin with (*cf.* Gadagkar and Gopinathan 1980, Figs. 4–5, Patel and Rao 1984, Fig. 1–2), subsequent analysis focusses on Case 3 that contains solely density-dependent absorption without any density dependence in burst size. That is, subsequent analysis focusses on Eq. 22 for $v(t+1)$ that assumes the burst size is proportional to m and that the absorption probability of a virus particle drops to zero as the virus/bacteria ratio, v, approaches the value, κ, at which all the binding sites on the bacteria are occupied.

Analysis of Model with Density-Dependent Absorption

Condition for Viral Increase when Rare.

The virus population can begin to infect the bacterial population if it can increase when rare. That is, if $v(t) \approx 0$, then $v(t+1) > v(t)$ if

$$v(t+1) = \lambda_0 \, v(t) \tag{23}$$

where

$$\lambda_0 = \frac{d\, v(t+1)}{d\, v(t)}|_{v(t)=0} > 1 \tag{24}$$

The λ_0 is the eigenvalue evaluated at $v(t) = 0$ and it works out to be

$$\lambda_0 = \frac{a_o \, b_o}{R} > 1 \tag{25}$$

The $R > 1$ is the condition for the bacteria to increase in the absence of the virus, which is greater than one by assumption. Therefore, if $a_o \, b_o > R > 1$ the virus can spread into a population of increasing bacteria. This condition means that the absorption probability times the burst size, which is the viral production per time step, must exceed the bacterial production per time step for the virus to spread when rare.

If the burst size, b_o, and R are given, then Eq. 25 implies that the absorption probability must exceed a minimum for the virus to spread. Putting $\lambda_0 = 1$ and solving for a_o, yields the minimum probability of absorption that permits the virus to spread,

$$a_{o,\min} = \frac{R}{b_o} \tag{26}$$

In the instance of the parameters in Table 2 where the burst size, b_o is 40 and R is 2, $a_{o,\min}$ works out to be 0.05. Hence a_o has been taken as 0.1 to be safely above the minimum. Given the burst size and the bacterial growth factor, if the absorption probability is less than $a_{o,\min}$ then the virus cannot spread into a growing population of bacteria.

Equilibrium Viral Density, $\hat{v}$

Given that both the virus and bacteria can increase when rare, they may come to the equilibrium at an intersection between the $v(t+1)$ curve and the $v(t+1) = v(t)$ line, as was illustrated in Figure 6. The point of intersection depends on the saturation density, κ. The FindRoot[] function in Mathematica is used to calculate the value of $\hat{v}$ at an intersection point. Figure 7 (left) shows the curve of $\hat{v}$ obtain in this way as a function of κ.

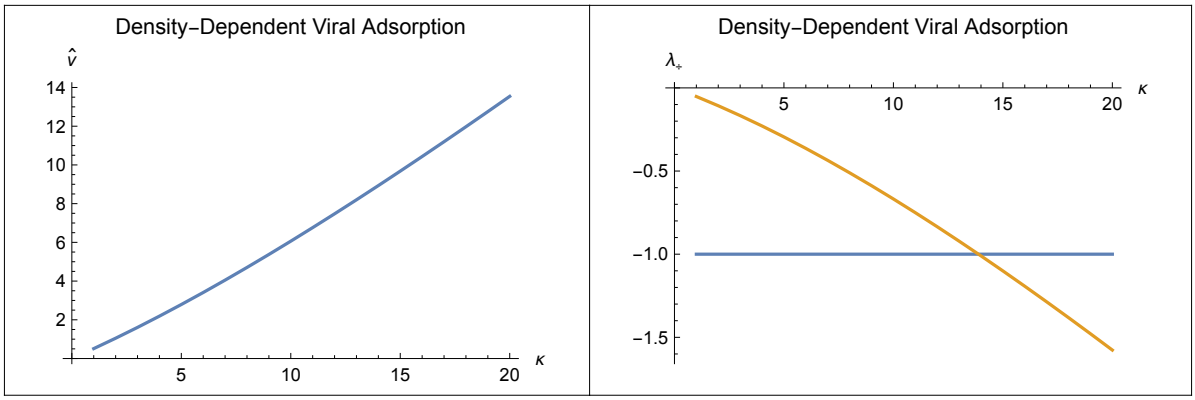

Figure 7: *Left: Equilibrium viral ratio, $\hat{v}$ as a function of κ. Right: Curve is eigenvalue evaluated at $\hat{v}$ as a function of κ and line at -1 marks the boundary between stable and unstable equilibria. The equilibria for κ below 14 are stable and characterized by a damped oscillatory approach whereas the equilibria for κ above 14 are unstable. Here, $a_o = 0.1$, $b_o = 40$, $R = 2$, and κ varies from 1 to 20.*

Stability of $\hat{v}$

The stability of an equilibrium viral ratio, $\hat{v}$, depends on λ_+ defined as

$$\lambda_+ = \frac{d\,v(t+1)}{d\,v(t)}\Big|_{v(t)=\hat{v}} \tag{27}$$

The λ_+ is the eigenvalue evaluated at a positive equilibrium point. If λ_+ is between $+1$ and -1 then the equilibrium is stable (*e.g.* Roughgarden 1996). Specifically, if λ_+ is between $+1$ and 0, the approach to equilibrium does not involve oscillations whereas if λ_+ is between -1 and 0, the approach to equilibrium involves damped oscillations.

Figure 7 (right) shows the curve of λ_+ as a function of κ. The λ_+ is always negative, so the approach to equilibrium is oscillatory. The horizontal line at -1 marks the boundary between stable and unstable equilibria. The horizontal line crosses the curve for λ_+ near $\kappa = 14$. Hence, the equilibria, $\hat{v}$, for $\kappa < 14$ are stable with an oscillatory approach. The equilibria for $\kappa > 14$ are unstable.

An additional source of density dependence may smooth the approach to equilibrium. Indeed, if density dependence in burst size is added and combined with the density dependence in absorption, then the eigenvalue may lie between 0 and $+1$, indicating a non-oscillatory approach to the equilibrium (not shown).

Trajectories

Figure 8 illustrates trajectories of both virus and bacteria for $\kappa < 14$. Trajectories illustrate the damped oscillations of $v(t)$ during the approach to a stable equilibrium. The trajectory of $N(t)$

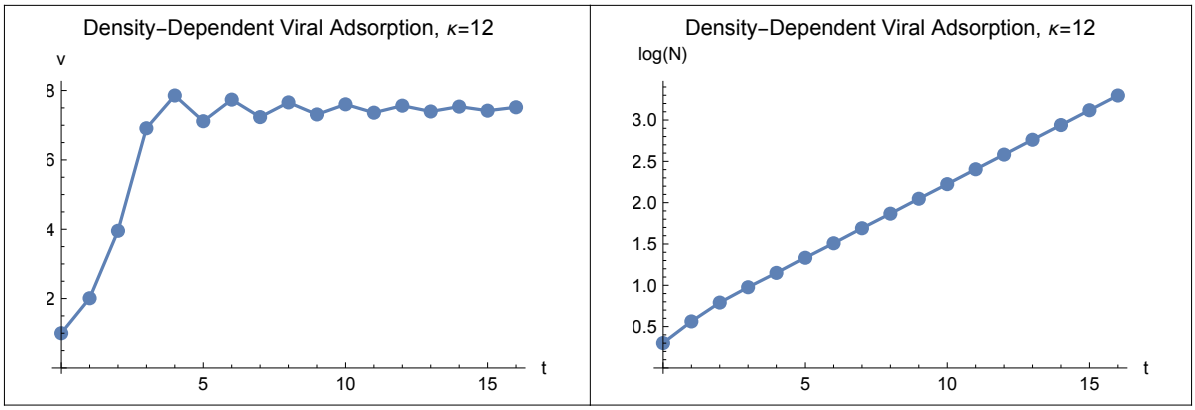

Figure 8: *Left: Trajectory of $v(t)$ showing damped oscillation during approach to equilibrium. Right: Trajectory of $\log_{10}(N(t))$ showing approach to exponential bacterial population growth. Here, $\kappa = 12$, $v(0) = 1$, $N(0) = 2$, $t_{\max} = 16$, $\kappa = 12$, $a_o = 0.1$, $b_o = 40$, $R = 2$ and $t_{\max} = 16$.*

also shows damped oscillations during the approach to the asymptotic growth factor, although the scale on the graph makes the oscillations difficult to see.

Figure 9 illustrates trajectories of both virus and bacteria for $\kappa > 14$. Trajectories illustrate a two-point limit cycle of $v(t)$ around the unstable $\hat{v}$. The trajectory of $N(t)$ also shows a two-point oscillation around the asymptotic growth factor although again, the scale on the graph makes the oscillations difficult to see.

The existence of a two-point limit cycle around the unstable equilibrium in Figure 9 is consistent with known dynamics for the discrete-time logistic equation (May 1976.) The possibility of more complex oscillations and chaotic trajectories with $\lambda_+ < -1$ remains to be explored. For the purposes of this paper, a comparison of the oscillations for this model in Figure 9 with those in Figure 1 shows that the oscillations in the present model are bounded from above and below whereas those in the Cambell (1961) model approach arbitrarily close to the axes, implying population extinction.

Infection Discount

Figures 8 and 9 show the bacterial population increasing with time. However, unlike these figures, the bacterial population does not necessarily increase even though the virus to bacteria ratio has reached a stable equilibrium, $\hat{v}$.

The net growth factor, R', for the bacteria per time step from Eq. 9 is $R' \equiv R\, e^{-\mu(t)}$. The R' must be greater > 1 for the bacterial population to increase. If the virus to bacteria ratio is at equilibrium, $\hat{v}$, then $\mu(t) = a_o\,(1 - \hat{v}/\kappa)\,\hat{v}$. In this situation,

$$R' = R\, e^{a_o\,(1-\hat{v}/\kappa)\,\hat{v}} \tag{28}$$

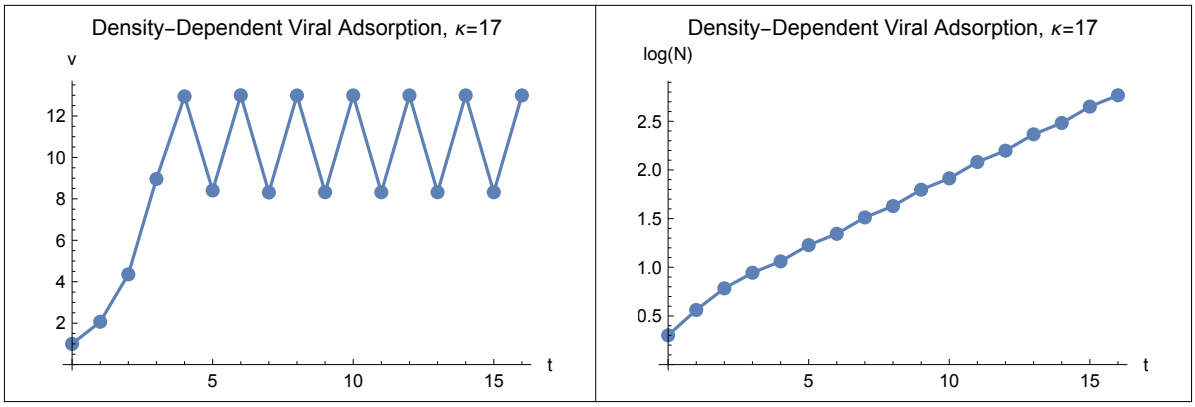

Figure 9: *Left: Trajectory of* $v(t)$ *showing a two-point limit cycle around the unstable equilibrium at* $\hat{v}$*. Right: Trajectory of* $\log_{10}(N(t))$ *showing a two-point oscillation in the exponential bacterial population growth. Here,* $\kappa = 17$*,* $v(0) = 1$*,* $N(0) = 2$*,* $t_{\max} = 16$*,* $\kappa = 12$*,* $a_o = 0.1$*,* $b_o = 40$ $R = 2$ *and* $t_{\max} = 16$*.*

Define the "infection discount", $I(R)$, as

$$I(R) \equiv e^{a_o\,(1-\hat{v}/\kappa)\,\hat{v}} \tag{29}$$

The infection discount indicates the degree to which the bacterial population growth factor is discounted as a result of the mortality caused by viral infections. The infection discount depends implicitly on R because $\hat{v}$ depends on R along with the other parameters. Hence, the bacteria can increase if

$$R\,I(R) > 1 \tag{30}$$

Figure 10 illustrates the infection discount for the parameters of Table 2. The discount becomes more severe as κ increases because $\hat{v}$ increases with κ. However, in the table, R is 2 and the discount never drops below $1/2$, so R' remains greater than one even as κ increases to 20. This indicates that the bacterial population can continue to increase for all levels of infection with the parameters of Table 2. Other parameters values (not explored) might not be so kind to the bacterial population.

Temperate Phage: Lytic to Lysogenic Transition

The preceding model for the population dynamics of virulent phage also applies to the lytic phase of a temperate phage. However, for the lysogenic phase of a temperate phage, a virus incorporates into a bacterium's genome and reproduces along with the bacterium itself as shown in Figure 4 (Right) . The main life-history question pertaining to temperate phage is when the phage should transition from lytic to lysogenic and from lysogenic back to lytic.

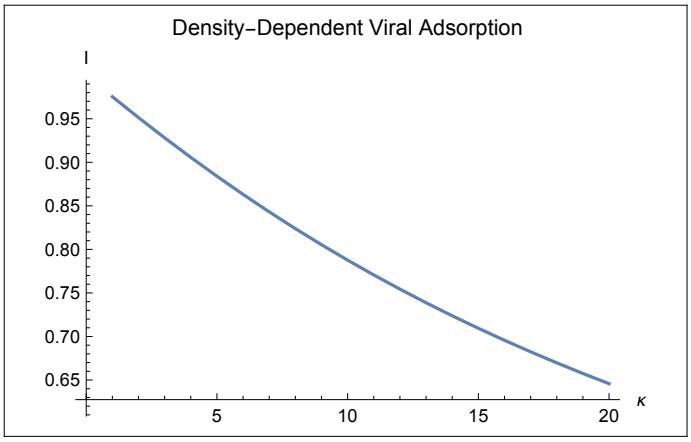

Figure 10: *Infection discount. Here,* $a_o = 0.1$, $b_o = 40$, $R = 2$ *and* κ *varies from 1 to 20.*

The answer to this question follows directly from the condition for virus to increase when rare, Eq. 25. The population dynamics of lysogenic phase is simply the same as that for the bacteria they reside in, namely, increasing by a factor of R each time step. On the other hand, the lytic phase can spread into the population of bacteria if $a_o\, b_o > R$, meaning that the initial absorption probability times the burst size must exceed the bacterial growth factor. So the lytic phase produces more virus per time step if if $a_o\, b_o > R$ whereas the lysogenic phase produces more virus per time step if $a_o\, b_o < R$. Thus, a switch function can be formulated as follows:

$$\begin{aligned} \text{A}: \quad a_o\, b_o &> R \quad - \text{ lytic phase best for virus} \\ \text{B}: \quad a_o\, b_o &< R \quad - \text{ lysogenic phase best for virus} \end{aligned} \tag{31}$$

Accordingly, various scenarios of environmental change can be envisioned that flip the switch from lytic to lysogenic or *vice versa*.

Intervention Affecting a_o with Hygienic Practice

If the access of virus particles to bacteria is sufficiently lowered by introducing air filters or other hygienic practices, then the best strategy switches from lytic to lysogenic. For example, the minimum value of a_o for the virus to spread in a bacteria population from Eq. 26 using the parameters in Table 2 works out to be 0.05. So if the hygienic practices reduce a_o below 0.05, the the virus should switch from lytic to lysogenic because doing so yields a higher viral population growth. This conclusion is consistent with the conclusion from Stewart and Levin (1984) that "lysogeny is an adaptation for phage to maintain their populations in 'hard times'." In this scenario, the virus are using the bacteria as a refuge.

Environmental Deterioration Affecting b_o and R Simultaneously

If a chemical such as a general toxin, pollutant or antibiotic is introduced into the environment, then whether the virus should switch from lytic to lysogenic depends on the relative impact of the chemical. For example, if the chemical is an antibiotic, then the bacterial growth factor, R, is lowered, say by 50%. Now, the viral burst size, b_o is likely affected too because, say, the ATP level and other resources within the bacteria drop, implying that fewer viral particles can be synthesized. If the viral burst size is also reduced by 50% as a result, the reductions to both virus and bacteria cancel out in the switch function, Eq. 32, leaving the lytic *vs.* lysogenic state unchanged. But if the chemical sufficiently affects b_o more than R, then the virus could switch from lytic to lysogenic and conversely, if the chemical affects R more than b_o. Thus, the idea of lysygeny offering a refuge for lytic virus to escape "hard times" when there is general environmental deterioration depends on the relative impact of the deterioration on the virus and on the bacteria.

Environmental Enhancement Affecting R—Microbialization

Overfishing and eutrophication on coral reefs leads to an increase in fleshy algae. The algae are largely ungrazed and produce an increase in dissolved organic carbon (DOC). The increase in DOC in turn leads to a replacement of the type of bacteria characteristic of low-nutrient environments (oligotrophs) with those typical of nutrient rich environments (copiotrophs). Forest Rohwer and colleagues (Haas *et al.* 2016) refer to this shift in coral reef ecosystem structure as "microbialization."

The increase in DOC from microbialization leads to an increase in microbial growth, R. The effect of increasing R in the switch function, Eq. 32, is to switch the virus from lytic to lysogenic, *i.e.* from state A to state B. This model therefore predicts that the microbialization resulting from increased DOC leads to an increase in lysgenic bacteria. More generally, this model predicts that the phage infecting oligotrophs are more likely to be lytic whereas those infecting copiotrophs are more likely to be lysogenic.

Lysogenic Conversion and Microbial Pathenogenicity

Rower and colleagues (Haas *et al.* 2016) further observe that the enrichment of copiotrophs during microbialization is correlated with an increase in virulence genes (Vega Thurber et al 2008) and that in turn is correlated with an increase in the prevalence of coral disease (Harvall *et al.* 1999). They conjecture that the pathogenicity of copiotrophs compared with that of oligotriophs is caused by lysogenic viruses accumulating in the copiotrophs that carry virulence genes for protection of their bacterial hosts. Through lysogenic conversion, the prophages in the copiotrophs

produce the virulence factors (Bondy-Denomy and Davidson 2014, Davies *et al.* 2016, Obeng *et al.* 2016).

This scenario is plausible according to the switch function of Eq. 32. whereby a lytic virus initially satisfying condition A in Eq. 32 switches to condition B if high DOH increases the bacterial R. Upon switching to B and incorporating into the bacterial genome as prophage, virulence genes become expressed. The virulence factors from these genes are of no direct value to the virus and its replication (morons), but by assumption, offer protection to their bacterial host. If so, the bacterial R increases because of this increased protection to a degree beyond that arising from the high DOH to begin with. However, the population growth of the virus as a prophage is exactly the same as that for the bacterium, namely, R. Any assistance the prophage supplies to its bacterial host such as increased protection exactly benefits it as well—no altruism is involved, merely an exact congruence of interests by both the viral prophage and its bacterial host.

Let the population growth for a bacterium infected with a prophage be $R^\star$, where $R^\star > R$, the bacterial growth in the absence of the prophage. Condition B in Eq. 32 then has R replaced by $R^\star$. Because $R^\star > R$ it is more difficult for the virulence-factor containing virus to switch back to the lytic condition, A, than if it were not carrying a virulence factor. Thus, once a virus incorporates as a prophage containing with a virulence or other gene benefiting the bacteria, it becomes locked into the lysogenic life cycle—it cannot revert to the lytic life cycle without giving up the $R^\star$ it now enjoys as a lysogen to obtain the lower R of a lytic virus.

The possibility that prophages become locked into the lysogenic life cycle because they contain a gene that benefits their bacterial host may explain the longevity of prophages in host genomes through evolutionary time (Hedžet *et al.* 2022, López-Leal *et al.* 2022).

Virus as Vectors of Horizontal Gene Transfer

Virus can bring about the horizontal transfer of genes (Canchaya et al 2003, Gilbert and Cordaux 2017, Borodovich et al 2022, Irwin et al 2022). Prophage in one bacterial line can "pick up" a gene-containing fragment of the host DNA (a moron), transition to the lytic phase, then infect other bacterial lines and ultimately transition back to a prophage in another bacterial line whereupon the foreign DNA is expressed there through lysogen conversion. The evolutionary question is why a virus should conveniently serve as a vehicle for transporting genes from one bacterial lineage to another.

The switch function, Eq. 32, suggests a scenario in which horizontal gene transfer makes evolutionary sense for the virus regardless of its effect on the bacteria. Suppose the bacterial environment is in continual fluctuation. If so, a high R supporting a lysogenic life cycle may fluctuate down to a low R favoring a lytic life cycle, whereupon the virus releases from the

bacterial genome and lyses into the environment as virions. Next, these particles infect other bacteria. If R should fluctuate back up to a high value favoring a lysogenic life cycle, then the newly infecting virus incorporate into the genome of their new hosts and express their gene-containing fragment by lysogen conversion.

This scenario derived from the model's switch function predicts that horizontal gene transfer should proceed at a higher rate in fluctuating environments than in quiescent environments.

Three-Level (Tripartite) Holobionts

Systems consisting of three levels—virus, bacteria and eukaryotic host, often called "tripartite" holobionts, are receiving increased attention (Moran et al 2005, Bordenstein et al 2006, Kelly et al 2014, Keen and Dantas 2018, Barr 2019, Belleghem et al 2019, Bodner et al 2021, Wahida et al 2021). A question raised by these contributions is whether a prophage gene expressed via lysogen conversion in a bacterium that resides in the microbiome of a eukaryotic host can improve the fitness of the eukaryotic host.

For viral-carried gene to affect the fitness of the host in a holobiont, a temperate virus must first be incorporated as a prophage into the bacterium—Eq. 32, Case B supplies the condition for this to occur. Next, the lysogenic bacterium must be incorporated into the host's microbiome. The process for entry into the host's microbiome is host-orchestrated species sorting (HOSS, Roughgarden 2023). By this process, the bacteria must offer enough benefit to the host to avoid its exclusion by the host immune response. If a gene in the prophage of a bacterium in the host's microbiome causes the bacterium to allocate sufficient resources to the host, then the host relaxes its immune screening of the bacterium and it becomes integrated in the host's hologenome forming a three-level symbiosis. Thus, a lysogen-converted gene in the prophage of a bacterium can theoretically contribute to holobiont fitness as a component of the hologenome provided the gene causes the bacterium it inhabits to contribute enough to the host fitness that it is allowed into the host's microbiome—the result is a functionally integrated tripartite holobiont.

Discussion

This paper has shown that the delay-differential equation model of Cambell (1961) for the population dynamics of virulent phage and bacteria should be set aside because its predictions of extreme virus-bacteria oscillations have been repeatedly falsified and the qualitative situation it describes whereby bacterial density dependence stabilizes unstable viral population growth simply does not occur.

This paper introduces a new and simple model for the population dynamics of phage and bacteria that features infection of bacteria by Poisson sampling of viral particles from the environ-

ment rather than mass-action collisions of virus with bacteria. Also, the new model is developed in discrete time with a time step equal to the viral latency period, rather than in continuous time.

Two sources of viral density dependence have been explored. Density-dependent burst size does not lead to virus-bacteria coexistence because the functional form of the density dependence suggested in the literature is not sufficiently strong. In contrast, density-dependent viral absorption onto the bacterial surface is sufficient to produce virulent virus-bacteria coexistence.

The model of virulent-phage bacteria population dynamics was extended to temperate phage. The condition for transition from a lytic to lysogenic phase was derived as a "switch function". The virus switches from lytic to lysogenic when its population grows faster with prophage than with separate virions produced by lysis of the infected cell. The switch function compares the product, (base absorption probability $\times$ the burst size), with the bacterial population geometric growth factor, R. The bacterial growth factor is used because the viral population growth factor when existing as prophage is identical to the bacterial population growth factor.

The switch function is used to predict temperate viral-bacteria dynamics in several environmental scenarios: intervention that lowers probability of absorption, environmental deterioration that affects both virus and bacteria, environmental enrichment that increases bacterial population growth (microbialization), fluctuating environmental conditions—this promotes horizontal gene transfer (HGT), and the integration of a prophage-containing bacteria population into the microbiome of a eukaryotic host thereby augmenting the hologenome with a fitness-enhancing gene and leading to a functionally integrated tripartite holobont.

Finding population-dynamic data for viruses has been challenging. The functional form for density-dependent absorption in this paper is surmised from kinetic studies carried out for other purposes. The molecular biology of viruses is increasingly well understood. Perhaps future research focussing more on ecological and evolutionary dimensions of virus biology will appear.

Acknowledgments

The author thanks Sergio Cobo-Lopez and Toni Luque for discussion of an early draft of this paper. This article is Contribution #2 from a project, The Theory of Holobiont Evolution, funded by the Gordon and Betty Moore Foundation through Grant GBMF10000 to the University of Hawaii.

References

Anderson, R. M. and May, R. M. 1979. "Population Biology of Infectious Diseases: Part I." Nature 280, 361–367.

Barr J. J. (2019). Missing a Phage: Unraveling Tripartite Symbioses within the Human Gut. mSystems, 4(3), e00105-19. https://doi.org/10.1128/mSystems.00105-19

Beretta, E. and Y. Kuang 1998. Modeling and analysis of a marine bacteriophage infection. Mathematical Biosciences 149 57–76

Beretta E. and Y. Kuang. 2001. Modeling and analysis of a marine bacteriophage infection with latency period. Nonlinear Anal Real World Appl 2:35–74.

Bjørnstad, Ottar 2018. Epidemics: Models and Data using R. Springer Nature Switzerland AG. https://doi.org/10.1007/978-3-319-97487-3

Bodner, Katie, Arin L. Melkonian, Markus W. Covert, 2021 The Enemy of My Enemy: New Insights Regarding Bacteriophage–Mammalian Cell Interactions, Trends in Microbiology, Volume 29, Issue 6, 2021, Pages 528–541, ISSN 0966-842X, https://doi.org/10.1016/j.tim.2020.10.014.

Bondy-Denomy, Joseph and Alan R. Davidson 2014. When a Virus is not a Parasite: The Beneficial Effects of Prophages on Bacterial Fitness. Journal of Microbiology (2014) Vol. 52, No. 3, pp. 235–242. DOI 10.1007/s12275-014-4083-3

Bordenstein SR, Marshall ML, Fry AJ, Kim U, Wernegreen JJ (2006) The tripartite associations between bacteriophage, Wolbachia, and arthropods. PLoS Pathog 2(5): e43. DOI: 10.1371/journal.ppat.0020043

Borodovich, T., Shkoporov, A. N., Ross, R. P., & Hill, C. (2022). Phage-mediated horizontal gene transfer and its implications for the human gut microbiome. Gastroenterology report, 10, goac012. https://doi.org/10.1093/gastro/goac012

Brown, Christopher M. and Kay D. Bidle. 2014. Attenuation of virus production at high multiplicities of infection in *Aureococcus anophagefferens*. Virology 466-467 (2014) 71–81. http://dx.doi.org/10.1016/j.virol.2014.07.023

Bull, J. J., J. Millstein, J. Orcutt and H. A. Wichman 2006. Evolutionary Feedback Mediated through Population Density, Illustrated with Viruses in Chemostats. The American Naturalist , Vol. 167, No. 2 pp. E39–E51 https://www.jstor.org/stable/10.1086/499374

Campbell, Allan. 1961. Conditions for the Existence of Bacteriophage. *Evolution* 15:153–165.

Campbell, Allan. 1981 Evolutionary Significance of Accessory DNA Elements in Bacteria, Ann. Rev. Microbiol. 35:55–83

Canchaya, C., Fournous, G., Chibani-Chennoufi, S., Dillmann, M. L., & Brüssow, H. (2003). Phage as agents of lateral gene transfer. Current opinion in microbiology, 6(4), 417–424. https://doi.org/10.1016/s1369-5274(03)00086-9

Davies, Emily V., Craig Winstanley, Joanne L. Fothergill and Chloe E. James 2016. The role of temperate bacteriophages in bacterial infection. FEMS Microbiology Letters, 363, 2016, fnw015. doi: 10.1093/femsle/fnw015

Diekmann, Odo, Hans Heesterbeek and Tom Britton 2013. Mathematical Tools for Understanding Infectious Disease Dynamics. Princeton University Press. Volume 7 in the series Princeton Series in Theoretical and Computational Biology
https://doi.org/10.1515/9781400845620

Dimitrov, D. 2004. Virus entry: molecular mechanisms and biomedical applications. Nat Rev Microbiol 2, 109–122 (2004). https://doi.org/10.1038/nrmicro817

Echeverría-Vega, A., Morales-Vicencio, P., Saez-Saavedra, C., Alvarez, M. A., Gordillo, F., Del-Valle, R., Solís, M. E., and Araya, R. (2020). Characterization of the Bacteriophage vB_VorS-PVo5 Infection on Vibrio ordalii: A Model for Phage-Bacteria Adsorption in Aquatic Environments. Frontiers in microbiology, 11, 550979.
https://doi.org/10.3389/fmicb.2020.550979

Ellis, E., and M. Delbrück. 1939. "The Growth of Bacteriophage." *J. General Physiology* 22:365–384. doi: 10.1085/jgp.22.3.365

Endy D, Kong D, Yin J. 1997 Intracellular kinetics of a growing virus: a genetically structured simulation for bacteriophage T7. Biotechnol Bioeng. Jul 20 55(2):375–89.

Foster-Nyarko, Ebenezer and Mark J. Pallen 2022 The microbial ecology of *Escherichia coli* in the vertebrate gut. FEMS Microbiology Reviews, 46, 1–22 DOI: 10.1093/femsre/fuac008

Gadagkar, Raghavendra and K. P. Gopinathan 1980 Bacteriophage burst size during multiple infections. J. Biosci., Vol. 2, Number 3, September 1980, pp. 253–259.

Gibson B, Wilson DJ, Feil E, Eyre-Walker A. 2018 The distribution of bacterial doubling times in the wild. Proc. R. Soc. B 285: 20180789. http://dx.doi.org/10.1098/rspb.2018.0789

Gilbert, C., & Cordaux, R. (2017). Viruses as vectors of horizontal transfer of genetic material in eukaryotes. Current opinion in virology, 25, 16–22. https://doi.org/10.1016/j.coviro.2017.06.005

Grove, Joe , Mark Marsh; 2011 The cell biology of receptor-mediated virus entry. J Cell Biol 26 December 2011; 195 (7): 1071–1082. doi: https://doi.org/10.1083/jcb.201108131

Haas, A., Fairoz, M., Kelly, L. *et al.* 2016. Global microbialization of coral reefs. Nature Microbiol 1, 16042. https://doi.org/10.1038/nmicrobiol.2016.42

Harvell CD, Kim K, Burkholder JM, Colwell RR, Epstein PR, Grimes DJ, Hofmann EE, Lipp EK, Osterhaus AD, Overstreet RM, Porter JW, Smith GW, Vasta GR. Emerging marine diseases—climate links and anthropogenic factors. Science. 1999 Sep 3;285(5433):1505-10. doi: 10.1126/science.285.5433.1505. PMID: 10498537.

Hedžet, Stina, Maja Rupnik & Tomaž Accetto 2022. Broad host range may be a key to long-term persistence of bacteriophages infecting intestinal Bacteroidaceae species. Scientific Reports 12:21098 https://doi.org/10.1038/s41598-022-25636-x

Huang, Gang, Yasuhiro Takeuchi, and Wanbiao MA. 2010. Lyapunov Functionals for Delay Differential Equations. Model of Viral Infections. Siam J. Appl. Math Vol. 70, No. 7, pp. 2693–2708

Hubbs NB, Whisby-Pitts MM, McMurry JL. 2019 Kinetic analysis of bacteriophage Sf6 binding to outer membrane protein a using whole virions. Acta Virol. 63(4):450-458. doi: 10.4149/av_2019_412. PMID: 31802688.

Huss, Phil, Anthony Meger, Megan Leander, Kyle Nishikawa and Srivatsan Raman (2021) Mapping the functional landscape of the receptor binding domain of T7 bacteriophage by deep mutational scanning eLife 10:e63775 https://doi.org/10.7554/eLife.63775

Irwin, N.A.T., Pittis, A.A., Richards, T.A. et al. Systematic evaluation of horizontal gene transfer between eukaryotes and viruses. Nat Microbiol 7, 327–336 (2022). https://doi.org/10.1038/s41564-021-01026-3

Keeling, M. J., & Rohani, P. (2008). Modeling infectious diseases in humans and animals. Princeton, NJ: Princeton University Press.

Keen, Eric C., Gautam Dantas, 2018 Close Encounters of Three Kinds: Bacteriophages, Commensal Bacteria, and Host Immunity, Trends in Microbiology, Volume 26, Issue 11, 2018, Pages 943–954, ISSN

Kermack, W. O. and McKendrick, A. G. 1927 "A Contribution to the Mathematical Theory of Epidemics." Proc. Roy. Soc. Lond. A 115, 700–721.

Kelly, Linda W., Gareth J. Williams, Katie L. Barott, Craig A. Carlson, Elizabeth A. Dinsdale, Robert A. Edwards, Andreas F. Haas, Matthew Haynes, Yan Wei Lima, Tracey McDole, Craig E. Nelson, Enric Sala, Stuart A. Sandin, Jennifer E. Smith, Mark J. A. Vermeij, Merry Youle, and Forest Rohwer. 2014. Local genomic adaptation of coral reef-associated microbiomes to gradients of natural variability and anthropogenic stressors. Proc. Nat. Acad. Sci. (USA) 111(28) 10227–10232. www.pnas.org/cgi/doi/10.1073/pnas.1403319111

Koehler, Melanie, Martin Delguste, Christian Sieben, Laurent Gillet and David Alsteens 2020. Initial Step of Virus Entry: Virion Binding to Cell-Surface Glycans. Annual Review of Virology 7:143–65 https://doi.org/10.1146/annurev-virology-122019-070025

Koonjan S, Cardoso Palacios C, Nilsson AS. Population Dynamics of a Two Phages–One Host Infection System Using Escherichia coli Strain ECOR57 and Phages vB_EcoP_SU10 and vB_EcoD_SU57. Pharmaceuticals. 2022; 15(3):268. https://doi.org/10.3390/ph15030268

Krysiak-Baltyn, Konrad , Gregory J. O. Martin, Anthony D. Stickland, Peter J. Scales, and Sally L. Gras 2016. Computational models of populations of bacteria and lytic phage. Crit Rev Microbiol, 2016; 42(6): 942–968 DOI: 10.3109/1040841X.2015.1114466

Levin, Bruce R. , Frank M. Stewart, and Lin Chao 1977 Resource-limited growth, Competition, and Predation: A model and Experimental Studies with Bacteria and Bacteriophage. Amer. Natur. 111:3–24.

López-Leal, Gamaliel, Laura Carolina Camelo-Valera, Juan Manuel Hurtado-Ramírez, Jérôme Verleyen, Santiago Castillo-Ramírez, Alejandro Reyes-Muñoza 2022. Mining of Thousands of Prokaryotic Genomes Reveals High Abundance of Prophages with a Strictly Narrow Host Range. mSystems 7:4 10.1128/msystems.00326-22.

Maginnis, Melissa S. 2018. Virus–Receptor Interactions: The Key to Cellular Invasion. J Mol Biol (2018) 430, 2590–2611 https://doi.org/10.1016/j.jmb.2018.06.024

May, Robert. 1976. Simple mathematical models with very complicated dynamics. Nature 261:459–467.

Moldovan, R., Chapman-McQuiston, E., and Wu, X. L. (2007). On kinetics of phage adsorption. Biophysical journal, 93(1), 303–315. https://doi.org/10.1529/biophysj.106.102962

Moran, Nancy & Degnan, Patrick & Santos, Scott & Dunbar, Helen & Ochman, Howard. (2005). The players in a mutualistic symbiosis: Insects, bacteria, viruses, and virulence genes. Proceedings of the National Academy of Sciences of the United States of America. 102. 16919–26. 10.1073/pnas.0507029102.

Obeng, Akbar, Adjie Pratama, and Jan Dirk van Elsas 2016. The Significance of Mutualistic Phages for Bacterial Ecology and Evolution. Trends in Microbiology, June 2016, Vol. 24, No. 6 http://dx.doi.org/10.1016/j.tim.2015.12.009

Parada, Verònica , Gerhard J. Herndl and Markus G. Weinbauer. 2006. Viral burst size of heterotrophic prokaryotes in aquatic systems. J. Mar. Biol. Ass. U.K. 86, 613–621

Patel, I. R. and K. K. Rao. 1984. Bacteriophage burst size as a function of multiplicity of infection. Current Science 53:198–200.

Philipson L. (1983). Attachment of viruses to cell receptors and penetration of viruses into cells. Textbook of Medical Virology, 51–56. https://doi.org/10.1016/B978-0-407-00253-1.50012-8

Prashant K. Purohit, Mandar M. Inamdar, Paul D. Grayson, Todd M. Squires, Janè Kondev, and Rob Phillips 2005 Forces during bacteriophage DNA packaging and ejection. Biophys J. Feb88(2):851–66. (p.852 caption to figure 1)

Prasith Baccam, Catherine Beauchemin, Catherine A. Macken, Frederick G. Hayden, and Alan S. Perelson 2006 Kinetics of Influenza A Virus Infection in Humans. Journal of Virlogy, Aug. 2006, p. 7590–7599 Vol. 80, No. 15 doi:10.1128/JVI.01623-05

Ranasinghe, Nilakshi 2019. Literature study of virus size, burst size, latent period and genome size across different lytic eukaryotic and prokaryotic virus groups—an overview of traits and possible trade-offs. MSc Thesis. Department of biology, University of Bergen

Roughgarden, J. 1996. Appendix A3: Matrix Algebra and Stability Theory. Pp. 556–581 in: Roughgarden. 1996. Theory of Population Genetics and Evolutionary Ecology, An Introduction. Prentice Hall, Upper Saddle River, NJ.

Roughgarden, J. 1998. *Primer of Ecological Theory*. Prentice Hall. New Jersey.

Roughgarden, J., S. F. Gilbert, E. Rosenberg, I. Zilber-Rosenberg, and E. Lloyd. 2018. Holobionts as units of selection and a model of their population dynamics and evolution. Biological Theory 13:44–65, https://doi.org/10.1007/s13752-017-0287-1.

Roughgarden, J. 2020. Holobiont evolution: mathematical model with vertical vs. horizontal microbiome transmission. Philosophy, Theory and Practice in Biology, 12:2. http://dx.doi.org/10.3998/ptpbio.16039257.0012.002.

Roughgarden, J. 2023. Holobiont Evolution: Population Theory for the Hologenome. The American Naturalist, https://doi.org/10.1086/723782.

Stewart, Frank M., and Bruce R. Levin 1984. The Population Biology of Bacterial Viruses: Why Be Temperate. Theoretical Population Biology. 26, 93-117 (1984)

Tang, X. H. and Xingfu Zou. 2008. Global Attractivity in a Predator-Prey System with Pure Delays. Proceedings of the Edinburgh Mathematical Society (2008) 51, 495–508 DOI:10.1017/S0013091506000988

Van Belleghem JD, Dabrowska K, Vaneechoutte M, Barr JJ, Bollyky PL. 2019 Interactions between Bacteriophage, Bacteria, and the Mammalian Immune System. Viruses. 2019; 11(1):10. https://doi.org/10.3390/v11010010

Vega Thurber, Rebecca L., Katie L. Barotta, Dana Halla, Hong Liua, Beltran Rodriguez-Muellera, Christelle Desnues, Robert A. Edwards, Matthew Haynesa, Florent E. Anglya, Linda Wegleya, and Forest L. Rohwer. 2008. Metagenomic analysis indicates that stressors induce production of herpes-like viruses in the coral *Porites compressa*. Proc. Nat. Acad. Sci. (USA) 105(47) 18413–18418. www.pnas.org/cgi/doi/10.1073/pnas.0808985105

Volterra, V. (1926). Variazioni e fluttuazioni del numero d'individui in specie animali conviventi. Mem. Acad. Lincei Roma. 2: 31–113.

Wahida, Adam, Fang Tang, Jeremy J. Barr, 2021 Rethinking phage-bacteria-eukaryotic relationships and their influence on human health, Cell Host & Microbe, Volume 29, Issue 5, 2021,Pages 681–688, ISSN 1931-3128,https://doi.org/10.1016/j.chom.2021.02.007.

Yamauchi, Yohei, Ari Helenius; Virus entry at a glance. 2013. J Cell Sci 15 March 2013; 126 (6): 1289–1295. doi: https://doi.org/10.1242/jcs.119685 0966-842X, https://doi.org/10.1016/j.tim.2018.05.009.

Supplementary Material

Terminology

A virus particle that infects a bacterium is a "bacteriophage" (eats bacteria) or just "phage", for short. A complete virus particle is a "virion"—it has a protein coat that is the "capsid" enclosing its nucleic acid genome.

A "virulent phage" enters a bacterial cell, commandeers its replication machinery and after a "latency period", releases copies of itself into the environment, killing the bacterium. "Lysis", from the Latin word for "a loosening", is the process by which the copies are released. The set of released copies is the "burst", the number of copies within the burst is the "burst size".

A "temperate phage" may either reproduce new virus particles for release into the environment while killing the bacterium *or* may integrate into the bacterium's genome and reproduce jointly with it. In the former case, the virus, like a virulent virus, commandeers the bacterium's replication machinery to produce copies of itself that after a latency period lyse from the bacterium killing it. This sequence is the "lytic pathway." In the later case, the virus integrates into the bacterial genome becoming a "prophage" that replicates along with the bacterial genome as the bacterium reproduces. The bacterium is not killed. A bacterium containing a prophage within it is a "lysogen". This sequence is the "lysogenic" pathway.

Following incorporation into a bacterium's genome, a temperate phage may either remain incorporated as a prophage during subsequent bacterial cell divisions. *Or*, it may become virulent by de-incorporating from the bacterium's genome and proceed to produce new virus particles by lysis into the environment while killing the bacterium it formerly resided in.

A prophage may augment a bacterium whose genome it resides in by providing the bacterium with a novel gene expressed through a process of "lysogen conversion" *i.e.*, the bacterium is converted from lacking a function into expressing a function. Prophages often encode "morons" that are not directly involved in viral replication and can confer a benefit to their bacterial host. Such genes are independent transcriptional units of DNA that are expressed while the phage is in the prophage state. Morons can include genes that enhance the virulence of their bacterial host with phage-encoded toxins.

Terms in virology are defined relative to experimental protocols that have no ready counterpart in ecology, hindering the translation of terms between these disciplines. Virologists define the "multiplicity of infection" or MOI with a protocol whereby phage are added to bacteria in a medium. The ratio of the number of phage to the number of bacteria initially added to the medium is the MOI. In this paper, $v(t) = V(t)/N(t)$, is the ratio of virus particles, $V(t)$, to bacteria, $N(t)$, in their source pools at time, t. Hence, the MOI roughly corresponds to $v(0)$ in this paper.

A "one-step growth curve" is a curve of viral abundance in continuous time from the time of absorption until the time of lysis. The one-step curve may include information about the abundance of virus both within the bacteria as well as in the media. A "multi-step growth curve" is an experimental iteration of the one-step curve obtained by allowing the experiment to run beyond the first step. In this paper, viral abundance, $V(t)$, and bacterial abundance, $N(t)$, are curves in discrete time and are recorded solely at the end of each latency period, not within the latency period. They refer to abundance in the environmental source pools, not to virus within bacteria during a time step. Furthermore, Gadagkar and Gopinathan (1980) define an "effective multiplicity of infection" as the "mean number of phages adsorbed per infected bacterium". They also define the "effective burst size" as the "mean number of phages liberated per phage adsorbed." In this paper, at each time step, m indexes the number of virus in a bacterium where $b(m)$ is the burst size from a bacterium infected with m virus, and although not used here, $b(m)/m$, would represent the effective burst size.

Stability Analysis of Campell Model with $\tau = 0$

The Jacobian matrix, J, with $\tau = 0$ evaluated at the equilibrium yields

$$J = \begin{pmatrix} \frac{-d\,r}{c\,K\,(b-1)} & -\frac{d}{b-1} \\ r\left(b - \frac{d}{c\,K} - 1\right) & 0 \end{pmatrix} \tag{32}$$

The eigenvalues of J, λ_1 and λ_2 are a pair of conjugate complex numbers the real part of which is

$$\Re(\lambda) = -\frac{d\,r}{2\,(b-1)\,c\,K} \tag{33}$$

Because $\Re(\lambda)$ is always negative, the equilibrium is always stable. And because the eigenvalues are complex, the trajectories reveal a virus-bacteria oscillation through time that winds in to the equilibrium point in a flow pattern representing a "stable focus". The period of the oscillation is approximately

$$T = \frac{e\,\pi}{\sqrt{d\,r}} \tag{34}$$

The period is determined by d and r, independent of b, c and K. The oscillation speeds up as d and/or r are increased.

Even though $\Re(\lambda)$ is always negative, its magnitude varies inversely with the bacterial carrying capacity, K. Hence, a high K diminishes the stability of the virus-bacterial equilibrium point. Indeed, if K is infinite, the equilibrium point is neutrally stable and the flow of trajectories represents a "center" as occurs in the original Volterra predator-prey model (Volterra 1926; for a summary *cf.* https://en.wikipedia.org/wiki/Lotka–Volterra_equations, retrieved July 28, 2022).

With the parameters of Table 1,

$$\Re(\lambda) = -3.08 \times 10^{-8} \tag{35}$$

$$T = 55.07 \text{ minutes} \tag{36}$$

The $\Re(\lambda)$ for these eigenvalues is nearly zero because k is 10^8 in Table 1 and thus the equilibrium is, practically speaking, neutrally stable.

Poisson Summation Identities

$$\sum_{m=1}^{\infty} P_m(\mu) = 1 - e^{-\mu} \tag{37}$$

$$\sum_{m=1}^{\infty} m\, P_m(\mu) = \mu \tag{38}$$